The 26th Iranian Conference on
Optics and Photonics (ICOP 2020),
and the 12th Iranian Conference on
Photonics Engineering and
Technology (ICPET 2020).
Kharazmi University,
Tehran, Iran,
Feb. 4-5, 2020

Kharazmi University

حسگری ضریب شکست به وسیله یک جاذب کامل باند- باریک مبتنی بر تشدیدهای پلاسمونی

زهرا مددی[1]، کامبیز عابدی[2]، غفار درویش[1] و مهدی خطیر[1]

[1]دانشکده مهندسی برق و کامپیوتر، دانشگاه آزاد اسلامی، واحد علوم و تحقیقات،تهران، ایران

[2]دانشکده مهندسی برق و کامپیوتر، دانشگاه شهید بهشتی،تهران، ایران

چکیده- در این مقاله یک جاذب کامل پلاسمونی مبتنی بر ساختار فلز-عایق-فلز بعنوان زیست حسگر طراحی شده است. طبق نتایج شبیه سازی‌های انجام شده با استفاده از روش عددی تفاضل محدود - حوزه زمان، پس از تابش عمود پرتو نور موج صفحه‌ای در محدوده طول موجی ۵۸۰ تا ۶۴۰ نانومتر، طیف جذب ساختار یک پیک تشدید باند باریک را نشان می‌دهد. با افزایش ضریب شکست آنالیت بر روی ساختار از n=1 تا n=1.1، طول موج تشدید از λ=600.1 nm به λ=614.8 nm جابجا خواهد شد. حساسیت، پهنای کامل در نیم ماکزیمم، و معیار شایستگی حسگر به ترتیب 147 nm/RIU، 9.6 nm و15.3 محاسبه شده است. تحلیل میدان الکتریکی در سطح مقطع‌های مشخصی از جاذب نشان می‌دهد، که تشدیدهای پلاسمونی در واسط‌های عایق – فلز و آنالیت- فلز تحریک می‌شوند، و با تقویت میدان در این سطوح، امکان حسگری در یک محدوده‌ی طول موجی بسیار کوچک فراهم می‌گردد.

کلید واژه- باند باریک، جاذب کامل پلاسمونیک، زیست حسگر، ضریب شکست، فلز- عایق- فلز.

Refractive Index Sensing by a Narrow-Band Perfect Absorber **base**d on Plasmonic Resonances

Zahra Madadi 1, Kambiz Abedi 2, Ghafar Darvish 1, and Mehdi Khatir1

1Department of Electrical and Computer Engineering, Science and Research Branch, Islamic Azad University, Tehran, Iran.

2 Department of Electrical and Computer Engineering, Shahid Beheshti University, Tehran, Iran. (k_abedi@sbu.ac.ir)

Abstract- In this paper, a plasmonic perfect absorber based on the metal-insulator-metal structure has been designed as a biosensor. Simulation results performed by the 3D FDTD numerical method show that the absorption spectrum of the proposed biosensor has a narrow-band resonance peak in the wavelength range of 580-640 nm. After the perpendicular incidence of a plane wave light within wavelength range mentioned, the resonance wavelength shifts from λ=600.1 nm to λ=614.8 nm when the analyte refractive index increases from *n*=1 to *n*=1.1. The sensor's sensitivity (S), full width at half maximum (FWHM) and the figure of merit (FOM) were obtained 147 *nm/RIU*, 9.6 nm, and 15.3, respectively. The analysis of the electric field at certain cross-sections of the absorber shows that the plasmonic resonances are stimulated at the insulator-metal and analyte-metal interfaces, and by amplifying the field at these surfaces, the sensing process is possible in the very small wavelength range.

Keywords: Meta-Insulator-Metal, Narrow-band, Plasmonic Perfect Absorber, Refractive Index, Biosensor;

1. Introduction

During recent years, plasmonic perfect absorbers (PPAs) as a subset of metamaterials have attracted much attention due to their applications in energy harvesting, detecting, and sensing [1]. The unit cell of the PPA devices usually composed of a metal-insulator-metal (MIM) structure so that an insulator layer would be sandwiched between two layers of metal. The upper metal layer is corresponding with the pattern of a metamaterial which becomes periodic through the repetition of the structure's unit cells within a certain order. The lower metal layer will be designed as a continuous sheet with a thickness higher than the penetration depth of incident wavelengths; and, it acts as a perfect mirror. In these structures, surface plasmon resonances (SPRs) and surface plasmon polaritons (SPPs) will be stimulated in insulator-metal interfaces [2,3]. The plasmonic perfect absorbers can be used as photonic biosensors. For example, PPAs based on a periodic array of metal nano-apertures with rectangular (or triangular) branches, cross-shaped apertures in the metal layer, metal circular holes, metal nano-bars, metal nano-discs, and dipole nano-antennas with additional arms have been suggested as biosensors [2-6]. In this paper, we present a new PPA design based on MIM structure which is used for refractive index sensing of analytes. The article is organized as follows: in section 2, the geometry and dimensions of the proposed sensors are described. The sensor performance evaluation is presented in Section 3. Section 4 covers the simulation results obtained for the plasmonic resonances characteristic. Finally, the paper is concluded in section 5.

2. **PPA** Sensor Structure Design

Figure 1 illustrates the unit cell of the proposed PPA structure so that two parallel silver (Ag) nano-blades are deposited on one dielectric spacer layer of Al_2O_3. A thin silver layer is also placed on the bottom of the structure as a perfect mirror. In this structure, the dielectric spacer causes the plasmonic coupling between SPR of the nano-blades and SPP of the bottom silver layer. In other words, the anti-parallel surface currents are excited in the nano-blades and bottom mirror and create a circulating current. Thus, the magnetic moment is attained that has a strong coupling with the magnetic component of the incident electromagnetic wave. Moreover, the accumulation of opposite charges at both ends of the blades forms an electric moment that has an interaction with the incident electric field. Thus, the electromagnetic energy is mostly confined in the small volume of the dielectric spacer.

The perfect absorption can be achieved by minimizing the reflectance dip intensity based on a rationally designing the structure dimensions. For this purpose, firstly the silver mirror thickness has been considered to be greater than the penetration depth of the incident wavelengths, to avoid any transmittance from the substructure. Secondly, the dielectric layer thickness has been selected to achieve maximum field localization in the spacer. The distance between two nano-blades is also considered to be so small that the maximum magnetic field confinement and strongest plasmonic coupling between them is achieved.

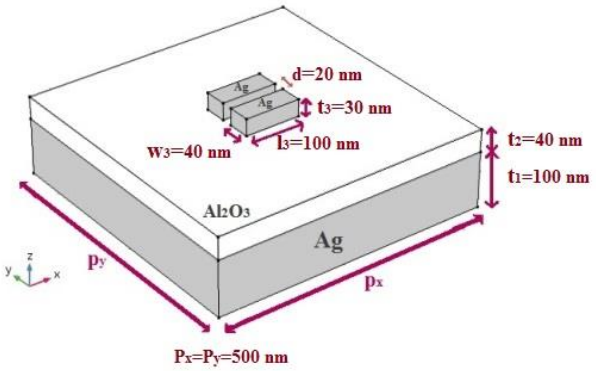

Fig. 1: The unit cell of the proposed PPA biosensor structure.

Accordingly, the thickness of the layers from bottom to top of the structure along the z-axis has been calculated as t_1=100 nm, t_2=40 nm, t_3=30 nm, respectively. The side length of the Al_2O_3 spacer and silver mirror along *x* and *y*-axes is considered to be P_x=P_y=500 nm. The length and width of the Ag blades have been adjusted to L_3=100 nm and W_3=40 nm, respectively. The gap between these two parallel blades is also considered to be d=20 nm.After designing the structure, a plane wave light along the *z*-axis and within 0.58-0.64 μm wavelength range will be illuminated vertically on the absorber surface, with an electric field polarization along the *x*-axis. The unit cell of the

sensor has been simulated through 3D FDTD numerical method (available from the Lumerical software package [11]). The simulation environment is limited from the up and down-sides by the perfectly matched layer (PML) boundary condition; and along *x* and *y*-axes, by the periodic boundary conditions. The dielectric constant of silver has been described through the Drude model, and the bulk plasma frequency, damping constant, and background dielectric constant have been calculated based on reference [7]. The refractive index of the Al_2O_3 layer is considered to be n=1.75 [8]. It is very important to note that, since silver metal has been used in the design of the proposed device, Its manufacturing cost is much lower than the gold-based absorbers.

3. Sensor Efficiency Evaluation

To evaluate the absorber performance, transmission, reflection, and absorption spectra of structure would be calculated. The Transmission spectrum would be suppressed completely by the silver mirror at the bottom of the structure ($T(\lambda)=0$). Reflection spectrum ($R(\lambda)$) is the intensity of power reflected from the overall absorber structure. Thus, the Absorption spectrum will be calculated through $A(\lambda) = 1-R(\lambda)$ [6]. Because of the dependence of the surface plasmon resonances on the adjacent dielectric refractive index, the resonance peak in the absorption spectrum shifts with changing analyte refractive index. To evaluate the sensor efficiency, the parameters of sensitivity and figure of merit are calculated as $S=\Delta\lambda/\Delta n$ and FOM= S/FWHM, respectively. Where, $\Delta\lambda$, Δn, and FWHM are the resonance wavelength shift, refractive index unit (RIU) variations and the full width at half maximum of the resonance peak, respectively [9,10].

4. Results and Discussions

In this step, the analyte liquids are poured onto the Al_2O_3 spacer up to a 40 nm height over it. After the illumination of vertical plane-wave light along the *z*-axis, the output absorption spectrum of structure for each of them has been measured and shown in figure 2(a). All spectra have a resonance peak with perfect absorbance above A=99.4%. The curve of the resonance peak wavelength variations versus the analyte refractive index has been plotted in Fig. 2(b).

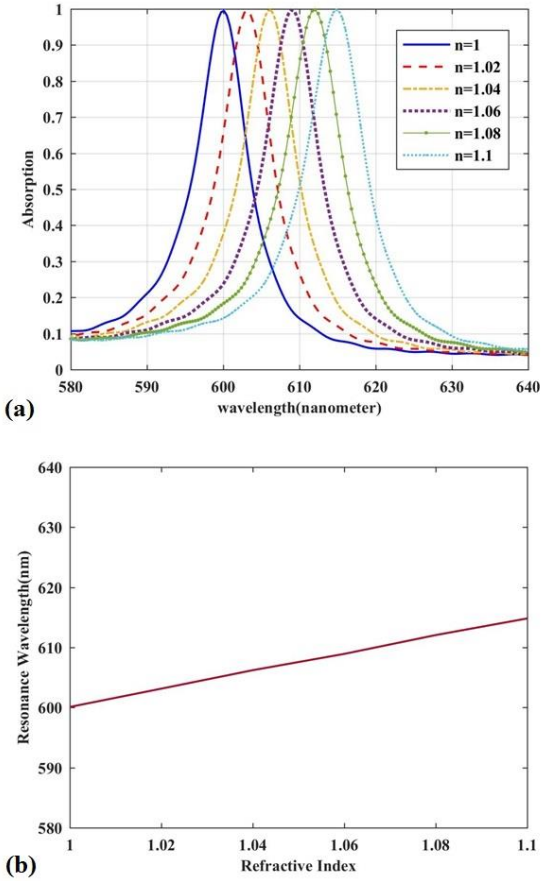

Fig. 2: (a)The structure absorption spectrum,(b) The resonance peak wavelength curve; for various refractive indices of the analyte.

It can be seen, the increasing of the analyte refractive index from *n*=1 to *n*=1.1 will result in a shift of resonance wavelength from λ=600.1 nm to λ=614.8 nm. Under this condition, sensitivity (S), FWHM, and FOM have been obtained as 147 *nm/RIU*, 9.6 nm, and 15.3, respectively. In another step, to show the occurrence of plasmonic resonances at metal-dielectric and metal-analyte interfaces, a 2D field monitor with *z*-*x* cutting plane (-20 nm<*z*<200 nm and -250 nm<*x*<250 nm) and another 2D field monitor with *z*-*y* cutting plane (-20 nm<*z*<200 nm and -250 nm<*y*< 250 nm) have been located at positions *y*=30 nm and *x*=0 nm, respectively. After the illumination of plane-wave light along the *z*-axis, the absolute value of electric field distribution has been computed at the

resonance wavelength in figure 3 ((a)for the first monitor in x=0 coordinates parallel to the z-axis, (b)for the second monitor in z=155 nm coordinates parallel to the y-axis). As can be seen, due to plasmonic resonances excitation, the electric field distribution is maximal at the dielectric-metal interfaces (z=0.14 µm and z=0.17 µm) and the analyte-metal blades interfaces (y=-0.05 µm and y=0.05 µm).

5. Conclusion

In this paper, a narrow-band PPA utilizing silver noble metal has been designed for analyte refractive index sensing which is much less expensive than gold-based sensors. The occurrence of plasmonic resonances at different interfaces of the structure and their coupling has led to the high field localization and the achievement of a very narrow resonance peak in the absorption spectrum of the device. Simulation results showed that the FWHM, sensitivity, and FOM have been obtained 9.6nm, 147 *nm/RIU*, and 15.3, respectively.

References

[1] C. Cao, Y. Cheng, "Quad-Band Plasmonic Perfect Absorber for Visible Light with a Patchwork of Silicon Nanorod Resonators", Materials.**11**(10),1954, 2018.

[2] Z. Madadi, K. Abedi, G. Darvish, M. Khatir, "An Infrared Narrow-band Plasmonic Perfect Absorber As Sensor", Optik.**183**, 670-676, 2019.

[3] Y. Li, B. An, S. Jiang, J. Gao, Y. Chen, S. Pan, "Plasmonic induced triple-band absorber for sensor application", OPTICS EXPRESS .**23**(13), pp.17607-17612, 2015.

[4] J. Ye, P.V. Dorpe, "Improvement of Figure of Merit for Gold Nanobar Array Plasmonic Sensors", Plasmonics Springer. **6**, pp.665-671, 2011.

[5] A.A. Jamali, B. Witzigmann, "Plasmonic Perfect Absorbers for Biosensing Applications", Plasmonics Springer. **9**, pp.1265-1270, 2014.

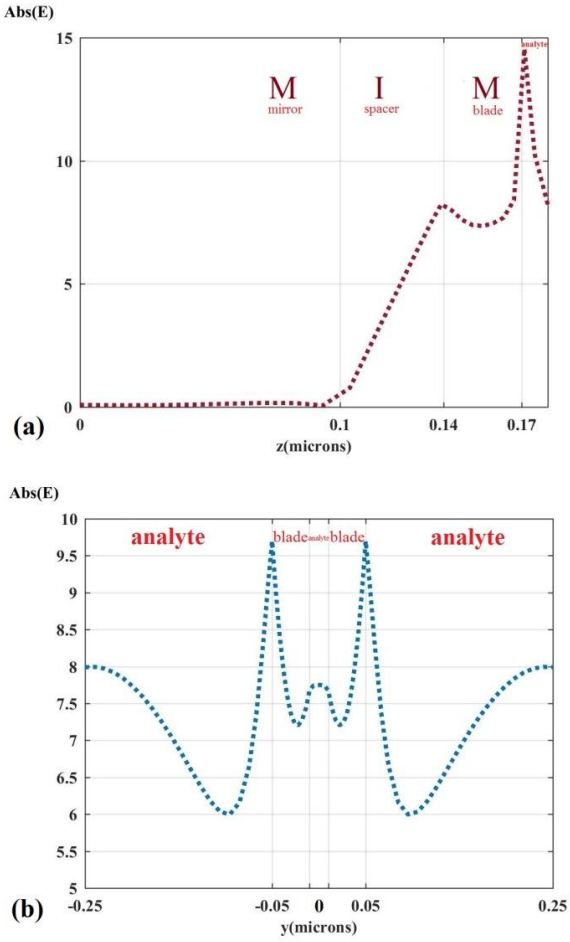

Fig. 3: The Abs(E) at resonance wavelength;(a) in x=0 and y=30 nm; (b) in x=0 and z=155 nm.

[6] S. Amiri, N. Nozhat, "Plasmonic nano-dipole antenna array with extra arms for sensing applications", OPTICAL PHYSICS. **33**(8), pp.1769-1776, 2016.

[7] M.A. Ordal, L.L. Long, R.J. Bell, S.E. Bell, R.R. Bell, R.W. Alexander, C.A. Ward, "Optical properties of the metals Al, Co, Cu, Au, Fe, Pb, Ni, Pd, Pt, Ag, Ti, and W in the infrared and far infra-red", Appl. Opt. **22**(7), pp.1099-1119, 1983.

[8] E.D. Palik, Handbook of Optical Constants of Solids Academic Press, 1998.

[9] J. Hammond, N. Bhalla, S. Rafiee, "Localized Surface Plasmon Resonance as a Biosensing Platform for Developing Countries", Biosensors. **4**, pp.172-188, 2014.

[10] P.N. Patel, V. Mishra, A.S. Mandloi, "Optical Biosensors: Fundamentals & Trends", Journal of Engineering Research and Studies (JERS). **I** (I), pp.15-34, 2010.

[11] Lumerical FDTD Solutions, https:// www.lumerical.com/tcad-products/fdtd/.